Biochimica et Biophysica Acta, 980 (1989) 209–219
Elsevier

BBA 74360

Synthesis and characterization of fluorescent Lucifer yellow-lipid conjugates

Eugene A. Nothnagel

Department of Botany and Plant Sciences, University of California, Riverside, CA (U.S.A.)

(Received 12 September 1988)
(Revised manuscript received 8 December 1988)

Key words: Fluorescent lipid; Fluorescent probe; Phospholipid; Sterol; Membrane probe; Lateral diffusion; Lucifer yellow-lipid conjugates

The syntheses of fluorescent lipid probes composed of Lucifer yellow dyes linked to either cholesterol or phospholipids are described. The spectral properties of these probes are characterized, and the probes are evaluated for use with model membranes and with live animal and plant cells. Of the probes synthesized, the cholesterol derivative is the easiest to prepare and appears to be the most useful because it readily labels the plasma membrane of live cells and maintains a high ratio of cell surface-to-cytoplasmic fluorescence.

Introduction

Hydrophobic fluorescent molecules have proven to be valuable probes for the characterization of a variety of membrane properties including surface charge, transmembrane potential, lipid fluidity, lipid lateral diffusion, and lipid metabolism [1]. In studies of model membranes and isolated biological membranes, many of the most useful probes have proven to be derivatives of anthracene, pyrene, 1,6-diphenylhexatriene, and other fluorophores that are excited with ultraviolet light. These probes are not so useful in studies of live cells because ultraviolet light often excites considerable autofluorescence and causes injury when applied to live cells.

A variety of fluorescent lipid probes that excite with visible light have been developed for use in studies of live cells. Most of these probes are either phospholipid derivatives or other molecules containing two hydrophobic chains. The properties of a number of these probes have been compared in studies involving model membranes [2,3] as well as live cells [4–6]. Many of these probes, including the widely-used carbocyanines and derivatized phosphatidylethanolamines, have chemical structures such that the probes are expected to insert into membranes in an orientation that positions the fluorophore portion of the probe in the polar region at the surface of the membrane. Another widely-used probe, 1-palmitoyl-2-(6-[*N*-(7-nitrobenz-2-oxa-1,3-diazol-4-yl)amino]caproyl)-*sn*-glycero-3-phosphocholine (NBD-PC), has the fluorophore located at the end of one of the fatty acyl chains. Although it has usually been assumed that NBD-PC incorporates in an orientation that positions the fluorophore deep in the nonpolar lipid region of the membrane, recent work has shown that the fluorophore is actually located in the polar region [7].

A smaller but increasing number of fluorescent sterols have also been used as membrane probes. For some of these probes, the sterol is made fluorescent by introducing conjugated double bonds into the sterol structure itself [8]. The other probes have been synthesized by attaching exogenous fluorophores to either the hydroxyl 'head' group [9,10] or the aliphatic 'tail' region [7,11] of cholesterol. These fluorescent sterols have been used in studies of lateral diffusion [12] and other properties [13]

Abbreviations: NBD-PC, 1-palmitoyl-2-(6-[*N*-(7-nitrobenz-2-oxa-1,3-diazol-4-yl)amino]caproyl)-*sn*-glycero-3-phosphocholine; $DC_{16:0}PE$, dipalmitoylphosphatidylethanolamine; $DC_{10:0}PE$, dilauroylphosphatidylethanolamine; $DC_{18:2}PE$, dilinoleoylphosphatidylethanolamine; $DC_{12:0}PC$, dilauroylphosphatidylcholine; $DC_{14:0}PC$, dimyristoylphosphatidylcholine; $DC_{16:0}PC$, dipalmitoylphosphatidylcholine; diO, 3,3'-dioctadecyloxacarbocyanine perchlorate; TLC, thin-layer chromatography; LY-Chol, dilithium 4-amino-*N*-[(*β*-(carbo(5-cholesten-3*β*-yl)oxy)hydrazinocarbonyl)amino]-1,8-naphthalimide-3,6-disulfonate; LY-$DC_{12:0}PE$, dilithium 4-amino-*N*-[3-(*β*-(dilauroyl-*sn*-glycero-3-phosphoethanolamino)ethylsulfonyl)phenyl]-1,8-naphthalimide-3,6-disulfonate; LY-$DC_{16:0}PE$, dipalmitoyl-analog of LY-$DC_{12:0}PE$; LY-$DC_{18:2}PE$, dilinoleoyl-analog of LY-$DC_{12:0}PE$; DMSO, dimethylsulfoxide.

Correspondence: E.A. Nothnagel, Department of Botany and Plant Sciences, University of California, Riverside, CA 92521, U.S.A.

of model membranes. Relatively little use of fluorescent sterols has been made in studies of live cells, although a 'head' group-labeled cholesterol has been used to study lateral diffusion in erythrocyte ghost membranes [14].

While a variety of fluorescent lipid probes have been introduced and characterized, problems often arise when these probes are used in studies on live cells. One such problem is inadequate levels of insertion into the membrane. The technique most often used to label live cells with fluorescent lipid probes involves incubating the cells in a medium into which a small aliquot of the lipid probe has been injected from a concentrated solution in an organic solvent, usually ethanol. An alternative technique involves incubating the cells in a medium containing small vesicles composed of unlabeled phospholipids and a small proportion of fluorescent lipid probe. The first technique, injection from a concentrated solution, has been used to achieve labeling of adequate intensity with carbocyanines [5,6,15], NBD-PC [6,15], fluorophores attached to a single hydrocarbon chain [6,15], and several other fluorescent lipid probes. The second technique, labeling from doped vesicles, appears to involve lipid exchange and is most effective with NBD-PC and related probes that have unmodified choline or ethanolamine headgroups [4]. It is not uncommon, however, to encounter cell types or lipid probes for which neither injection from a concentrated solution nor exchange from doped vesicles will achieve appreciable labeling of the cells. This problem has stimulated research on other labeling techniques, such as use of surfactants to catalyze insertion of fluorescent lipid probes into membranes [16].

A second problem that typically arises with fluorescent lipid probes involves localization of the probe in the labeled cells. For measurements of lateral diffusion and other studies of the plasma membrane, it is preferable that the fluorescent lipid probes insert and remain localized in the plasma membrane. Many lipid probes, however, rapidly internalize to label organelle membranes or other components of the cytoplasm of live cells. This problem is often noted in published studies of lateral diffusion in the plasma membrane [4,5,15,17] and has been documented through measurements of fluorescence lifetimes [18]. For some probes, internalization to the cytoplasm probably occurs by a simple permeability mechanism. With 1,6-diphenylhexatriene, for example, internalization can be alleviated if the probe is synthesized in a modified form containing a strong positive charge that reduces solubility in nonpolar environments [19]. Internalization of some other fluorescent lipid probes, however, is metabolically driven [20–22] and has been studied to elucidate transport and metabolic pathways of lipids in living cells [23,24].

The present study was undertaken with the goal of synthesizing and characterizing new fluorescent lipid probes for the plasma membrane of live cells. In particular the goal was to develop probes that would readily insert into the plasma membrane and then remain localized there with relatively little internalization to the cytoplasm. The strategy was to synthesize conjugates between lipids and Lucifer yellow dyes. Lucifer yellow CH and Lucifer yellow VS are highly fluorescent dyes that were originally synthesized for use in dye-coupling studies of cell-to-cell transport [25]. The chemical structures of both dyes include two highly-charged sulfonate groups that render the dyes very water soluble and virtually membrane impermeant [25]. Both dyes also contain reactive groups that enable the dyes to be covalently linked to macromolecules [26]. These two features have enabled the attachment of Lucifer yellow CH to the surface of live animal cells [27] and the attachment of both Lucifer yellow CH and Lucifer yellow VS to the surface of live plant protoplasts [28]. Lucifer yellow CH has been linked to oxidized ganglioside to form a fluorescent glycolipid probe [29].

Materials and Methods

Lucifer yellow CH was from Aldrich (Milwaukee, WI, U.S.A.), Sigma (St. Louis, MO, U.S.A.), Research Organics (Cleveland, OH, U.S.A.), or Molecular Probes (Eugene, OR, U.S.A.), with products from all suppliers giving similar results. Lucifer yellow VS, cholesterol, and dipalmitoylphosphatidylethanolamine ($DC_{16:0}PE$) were from Sigma. Cholesteryl chloroformate was from Aldrich or Steraloids (Wilton, NH, U.S.A.). Dilauroylphosphatidylethanolamine ($DC_{12:0}PE$), dilinoleoylphosphatidylethanolamine ($DC_{18:2}PE$), dilauroylphosphatidylcholine ($DC_{12:0}PC$), dimyristoylphosphatidylcholine ($DC_{14:0}PC$), dipalmitoylphosphatidylcholine ($DC_{16:0}PC$), and NBD-PC were from Avanti Polar Lipids (Birmingham, AL, U.S.A.). Molecular Probes was the supplier of 3,3'-dioctadecyloxacarbocyanine perchlorate (diO). All solvents were of reagent grade.

Two types of thin-layer chromatography (TLC) plates (5 × 20 cm), K6F silica gel and KC18F reversed phase, were obtained from Whatman Chemical Separation (Clifton, NJ, U.S.A.).

Syntheses

(A) Cholesterol probe. Fig. 1A shows the chemical structure of dilithium 4-amino-*N*-[(β-(carbo(5-cholesten-3β-yl)oxy)hydrazinocarbonyl)amino]-1,8-naphthalimide-3,6-disulfonate (LY-Chol). This probe was synthesized by a one-step reaction of Lucifer yellow CH with cholesteryl chloroformate, a reaction similar to that described by Barak [30] for the synthesis of a fluorescein derivative of cholesterol. Lucifer yellow CH (34.3 mg, 75 μmol) was added to 1.5 ml of dimethylformamide and then stirred at 23°C. After the dye was completely dissolved, 1.5 ml of pyridine was added. To this 3.0 ml of dye solution was added 0.75 ml of a

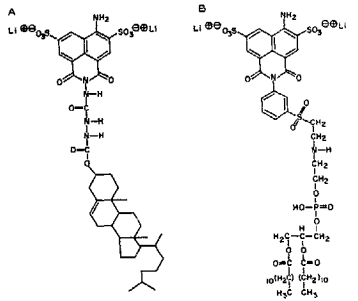

Fig. 1. Expected chemical structures of the fluorescent Lucifer yellow-lipid conjugates synthesized in this work. (A) LY-Chol. (B) LY-$DC_{12:0}$PE. The other two phospholipid probes, LY-$DC_{16:0}$PE and LY-$DC_{18:2}$PE, differ from LY-$DC_{12:0}$PE only in the fatty acyl chains.

dichloromethane solution containing 67.4 mg (150 μmol) of cholesterol chloroformate. After the reaction vial was purged with nitrogen gas, the mixture was stirred for 24 h in the dark at 23°C. The solvent was then removed at 60°C by evaporation under a stream of nitrogen gas to leave a syrupy residue. Excess cholesteryl chloroformate was removed from the residue by first extracting four times with 10-ml aliquots of dichloromethane and then suspending and partitioning the remaining solids in a two-phase system composed of 8 ml of water and 2 ml of dichloromethane. The aqueous phase was retained and washed with another 4 ml of dichloromethane. The resulting aqueous phase was collected and reduced to a volume of 4 ml by evaporation at 60°C under a stream of nitrogen gas. To this 4 ml solution was added 8 ml of *n*-butanol. After mixing and phase separation, the upper, butanol-rich phase was separated and retained. Three further partitions of the lower phase were performed, each partition involving the addition of 1.5 ml of water and 8 ml of *n*-butanol, with subsequent removal and retention of each upper phase. At the conclusions of the four partitions, the lower, water-rich phase contained mostly unreacted Lucifer yellow CH and was discarded. The four upper phases that were retained were pooled and washed one final time by the addition of a few ml of water to form a small lower phase which was discarded. The upper phase was evaporated to dryness, resuspended in 6 ml of water, and lyophilized for storage. Yield was 48 μmol (64%).

Analysis of the product by TLC on K6F silica gel plates was performed with dichloromethane/methanol/water (65:30:5, v/v/v) as the solvent. LY-Chol migrated with $R_f = 0.56$ in this system. When excited with long-wavelength ultraviolet light, LY-Chol fluorescence changed color from yellow to orange as the solvent evaporated from the plate after development (see Results). This property facilitated identification of the LY-Chol spot, since unreacted Lucifer yellow CH and most other unidentified components in the reaction mixture fluoresced yellow on silica gel under both wet and dry conditions. When analyzed by TLC on KC18F reversed-phase plates with methanol/water (80:20, v/v) as the solvent, LY-Chol migrated with $R_f = 0.65$ and fluoresced yellow on both wet and dry plates. On both silica gel and reversed-phase TLC, the final LY-Chol preparation appeared to be at least 90% pure. Of the trace impurities present, the largest appeared at $R_f = 0.60$ on the K6F plates. Since this trace impurity also exhibited a fluorescence change from yellow to orange as the plate dried, it may have been an isomer or other structural relative of LY-Chol.

(B) Phospholipid probes. Fig. 1B shows the chemical structure of dilithium 4-amino-*N*-[3-(β-(dilauroyl-*sn*-glycero-3-phosphoethanolamino)ethylsulfonyl)phenyl]-1,8-naphthalimide-3,6-disulfonate (LY-$DC_{12:0}$PE). This probe and its dipalmitoyl- and dilinoleoyl-analogs (LY-$DC_{16:0}$PE and LY-$DC_{18:2}$PE, respectively) were synthesized by a one-step reaction of the vinyl sulfone group of Lucifer yellow VS [25,26] with the primary amine of the respective phosphatidylethanolamine. The synthesis of LY-$DC_{12:0}$PE was typical of the syntheses of all three of these probes. Lucifer yellow VS (41.3 mg, 75 μmol) was added to 6 ml of pyridine, stirred and warmed at 60°C until fully dissolved, and then cooled to 23°C. To this solution was added 3 ml of a chloroform solution containing 43.4 mg (75 μmol) of $DC_{12:0}$PE. After the reaction vial was flushed with nitrogen gas and sealed, the reaction mixture was stirred overnight at 23°C in the dark. The solvent was then removed by evaporation at 23°C under a stream of nitrogen gas. The residue was mixed with 5 ml of *n*-butanol and 2 ml of water. During phase separation of this mixture, most of the unreacted Lucifer VS, some unidentified dye components, and about 30% of the LY-$DC_{12:0}$PE partitioned into the lower phase, which was removed and discarded. The upper phase was mixed with 2 ml of water. After this mixture separated, the lower phase was removed and saved. Three further partitions of the upper phase were performed, each involving the addition of 2 ml of water and 0.5 ml of *n*-butanol. Each lower phase that formed was removed and pooled with the previous lower phases. The final upper phase contained essentially all of the unreacted $DC_{12:0}$PE and was discarded. The four pooled lower phases were concentrated to a volume of 1 ml by evaporation at 60°C under a stream of nitrogen gas. This 1 ml was mixed with 3 ml of *n*-butanol. During this final phase separation, the remaining unreacted

Lucifer yellow VS and about 10% of the LY-$DC_{12:0}$PE partitioned into the lower phase, which was removed and discarded. The upper phase was evaporated to dryness and then redissolved in 3 ml of chloroform/methanol (2:1, v/v) for storage. Yield was 15 μmol (20%).

The phospholipid probes were analyzed by TLC on the same plates and solvent systems as described above for the cholesterol probe. On K6F silica gel plates, the phospholipid probes migrated with $R_f = 0.51$ to 0.57, and all three probes exhibited a change in fluorescence color form yellow to orange as the solvent evaporated from the plates. Only LY-$DC_{16:0}$PE and LY-$DC_{18:2}$PE were tested on the KC18F reversed-phase plates. These two probes migrated with $R_f = 0.64$ and fluoresced yellow on both wet and dry plates. All three probes were approximately 90% pure, as judged from appearance on TLC.

Analytical instrumentation and methods

(A) Mass spectrometry. Fast atom bombardment-mass spectrometry was performed with a VG Analytical ZAB-1FHF mass spectrometer (Danvers, MA, U.S.A.) using xenon as the bombarding gas and 8 kV as both the gun and accelerating voltages. The specimen matrices were glycerol for LY-Chol and thioglycerol for the phospholipid probes. Both positive- and negative-ion modes were used, with the negative-ion mode giving the stronger spectra.

(B) Absorption spectroscopy. Absorption spectra were recorded with a Beckman DU-6 spectrophotometer (Fullerton, CA, U.S.A.). Published absorption coefficients at the peak of the long wavelength absorption bands are $\epsilon_{428} = 11\,900\ M^{-1} \cdot cm^{-1}$ for Lucifer yellow CH and $\epsilon_{428} = 12\,200\ M^{-1} \cdot cm^{-1}$ for Lucifer yellow VS when the dyes are dissolved in water [26]. As determined by comparing absorbances in water with absorbances in other solvents, the absorption coefficient of Lucifer yellow CH in isopropanol/water (1:1, v/v) is $\epsilon_{430} = 11\,700\ M^{-1} \cdot cm^{-1}$, and the absorption coefficient of Lucifer yellow VS in chloroform/methanol (2:1, v/v) is $\epsilon_{430} = 11\,200\ M^{-1} \cdot cm^{-1}$. Concentrations of solutions of the fluorescent lipid probes were determined from absorbances by assuming that absorption coefficients for the linked dyes were the same as for the free dyes, and by using the molecular weights of the fluorescent lipid probes (869.91 for LY-Chol, 1130.21 for LY-$DC_{12:0}$PE, 1242.37 for LY-$DC_{16:0}$PE, and 1290.48 for LY-$DC_{18:2}$PE).

(C) Fluorescence spectroscopy. Fully-corrected excitation and emission spectra were recorded on a Spex Fluorolog 2 model 112A spectrofluorometer (Edison, NJ, U.S.A.). Temperature control of the specimen was achieved through use of a jacketed cuvette holder connected to a water bath circulator. The specimen was magnetically stirred, and the temperature was measured with a thermocouple inserted directly into the cuvette. Quantum yield determinations were performed by the method of Guilbault [31] with fluorescein in 0.1 M NaOH as a standard of quantum yield 0.92 [32].

Fluorescence lifetime determinations were made by the single-photon counting technique using an EEY Scientific nanosecond fluorimeter (La Jolla, CA, U.S.A.) with a high-pressure hydrogen arc lamp. The measurements were performed by David A. Johnson (Division of Biomedical Sciences, University of California, Riverside), as described [33].

(D) Fluorescence microscopy. Labeled cells were examined with an American Optical/Reichert epifluorescence microscope (Buffalo, NY, U.S.A.) using violet (435.8 nm) excitation light from a mercury arc lamp. The objective lenses were brightfield achromats; 100X, 1.25 numerical aperture for erythrocyte ghosts and 45X, 0.66 numerical aperture for the other cell types. Micrographs were recorded on Kodak Tri-X film with 9 min development in Kodak D-19 developer.

(E) Fluorescence photobleaching recovery. Lateral diffusion of the fluorescent lipid probes in membranes was monitored by spot fluorescence photobleaching recovery, as described by Axelrod et al. [34]. Our instrument for performing these measurements has been described in detail elsewhere [35] and is similar to the instrument described by Bloom and Webb [36]. Temperature control of the specimen was achieved through use of a jacketed microscope stage connected to a water bath circulator. Temperature was measured with a thermocouple bonded to the upper surface of the microscope slide. Recovery curves were analyzed by least-squares fitting to the models of Axelrod et al. [34]. Reported diffusion coefficients and mobile fractions are averages with standard deviations.

Preparation of lipid vesicles

Two classes of lipid vesicles were prepared for use in this project. Small (mostly 1 to 5 μm diameter) multilamellar vesicles were used in studies of fluorescence lifetimes and fluorescence excitation/emission spectra. These vesicles were prepared in a buffer (150 mM NaCl, 10 mM sodium phosphate, pH = 7.2) by the method of Alecio et al. [12] and were composed of 5 mol% cholesterol and 95 mol% $DC_{14:0}$PC. During vesicle preparation, LY-Chol (0.05 mol%), LY-$DC_{16:0}$PE (0.1 mol%), or LY-$DC_{18:2}$PE (0.1 mol%) was added to the lipid mixture.

Large (10 to 50 μm diameter) multilamellar vesicles were used in the fluorescence photobleaching recovery experiments. Vesicles of four different lipid compositions were prepared in distilled and deionized water by the method of Fahey and Webb [37]. The lipid compositions were 10 mol% $DC_{12:0}$PC, 100 mol% $DC_{16:0}$PC, 50 mol% $DC_{12:0}$PC and 50 mol% $DC_{16:0}$PC, or 90 mol% $DC_{14:0}$PC and 10 mol% cholesterol. During ves-

icle preparation, 0.05 mol% of LY-Chol or LY-$DC_{18:2}$PE was added to the lipid.

Labeling and isolation of erythrocyte ghosts

Acid-citrate-dextrose human blood was a gift of Irwin W. Sherman and Esther Valdez (Department of Biology, University of California, Riverside). Erythrocytes were isolated from the blood by the method of Bennett [38] and then washed as described by Golan et al. [14]. For fluorescence microscopy and fluorescence photobleaching recovery experiments, the washed erythrocytes (0.6 ml of 0.12 hematocrit) were labeled by the addition of 50 μg/ml LY-Chol (from 10 mg/ml stock in isopropanol/water (1:1, v/v)), 400 μg/ml LY-$DC_{18:2}$PE (from 20 mg/ml stock in dimethylsulfoxide (DMSO)), 400 μg/ml LY-$DC_{16:0}$PE (from 20 mg/ml stock in DMSO), or 150 μg/ml diO (from 10 mg/ml stock in acetone). After labeling had proceeded for 20 min at 24°C, the labeled erythrocytes were washed once by centrifugation and then lysed and washed to obtain ghosts as described by Golan et al. [14].

For quantitation of the amount of labeling by LY-Chol, aliquots of washed erythrocytes (2 ml of 0.15 hematocrit) were labeled as above with LY-Chol at various concentrations up to 100 μg/ml. After lysis and washing, the labeled ghosts were resuspended in 1 ml of water. Lipids were extracted from a portion (0.5 ml) of each labeled ghost preparation by the method of Roelofsen and Ott [39], and total sterols in the extract were quantitated by the colorimetric assay of Kates [40] with cholesterol as the standard. The level of LY-Chol incorporated into the ghosts was quantitated by adding a 0.2 ml aliquot of a labeled ghost preparation to 4.8 ml of a buffer composed of 4% (w/v) sodium dodecylsulfate, 50 mM sodium phosphate (pH 7.0) and then using the spectrofluorometer to measure the intensity of fluorescence from the solution. A standard curve to convert fluorescence intensity to mol of LY-Chol was prepared by measuring the intensity of fluorescence from a solution of unlabeled ghosts after buffer and known quantities of LY-Chol were added.

Labeling of tissue culture cells

Human amelanotic melanoma cells (American Type Culture Collection CRL 1585) were grown on microscope coverslips in fetal calf serum-supplemented medium by Esther Valdez and Irwin W. Sherman (Department of Biology, University of California, Riverside). The cells were washed twice with Hanks' balanced salt solution (without phenol red; GIBCO Laboratories, Grand Island, NY, U.S.A.) and then placed in Medium 199 (without phenol red; GIBCO) in preparation for labeling. Labeling was initiated by adding 10 μg/ml NBD-PC (from 2 mg/ml stock in ethanol), 200 μg/ml LY-$DC_{18:2}$PE (from 20 mg/ml stock in DMSO), 200 μg/ml LY-$DC_{16:0}$PE (from 20 mg/ml stock in DMSO), or 10 or 50 μg/ml LY-Chol (from 10 mg/ml stock in isopropanol/water (1:1, v/v)). After incubating with the fluorescent lipid probe for 20 min at 26°C, the cells were washed 3 times with Hanks' balanced salt solution, once with Medium 199, and then mounted in Medium 199 for photography and fluorescence photobleaching recovery experiments.

Isolation and labeling of plant protoplasts

Protoplasts were isolated from the cortex of the primary root of maize (*Zea mays* L. A632) seedlings by the method of Gronwald and Leonard [41]. The protoplasts were suspended in 0.7 M mannitol, and labeling was initiated by adding 50 μg/ml LY-Chol (from 10 mg/ml stock is isopropanol/water (1:1, v/v)). After incubating with the fluorescent lipid probe for 20 min at 26°C, the protoplasts were washed three times by centrifugation in 0.7 M mannitol.

Results

Spectra obtained by fast atom bombardment-mass spectrometry (Fig. 2) were consistent with the expected chemical structures of the Lucifer yellow-lipid conjugates (Fig. 1). A strong spectrum was readily obtained for LY-Chol and showed a molecular ion for LY-Chol as the dominant peak in the spectrum (Fig. 2A). Spectra were much more difficult to obtain for LY-$DC_{16:0}$PE and LY-$DC_{18:2}$PE. Signals in the ranges expected for the molecular ions of these phospholipid probes could be observed only transiently, since they rapidly degraded during observation. An analogous phospholipid probe, LY-$DC_{12:0}$PE, was synthesized with shorter fatty acyl chains because of the expectation that a stronger mass spectrum might be obtained. This expectation was fulfilled, as evidenced by the spectrum of Fig. 2B. Since the high mass signals degraded rapidly even for this probe, however, it was necessary to use multichannel averaging to obtain strong molecular ion peaks.

Spectral properties of the probes

The ultraviolet-visible absorption spectrum (not shown) of LY-Chol is isopropanol/water (1:1, v/v) contains principal maxima at 282 nm and 430 nm. Absorption spectra (not shown) of LY-$DC_{16:0}$PE and LY-$DC_{18:2}$PE in chloroform/methanol (2:1, v/v) both contain principal maxima at 277 nm and 432 nm. As expected, these absorption maxima are very similar to those of the precursor dyes, Lucifer yellow CH and Lucifer yellow VS [26].

Solvent effects on the long-wavelength absorption and emission properties of LY-Chol and LY-$DC_{18:2}$PE are summarized in Table I. While the emission maxima of many dyes tend to shift toward shorter wavelengths as the solvent polarity decreases [1,10,11], the emission maxima of both LY-Chol and LY-$DC_{18:2}$PE tend to

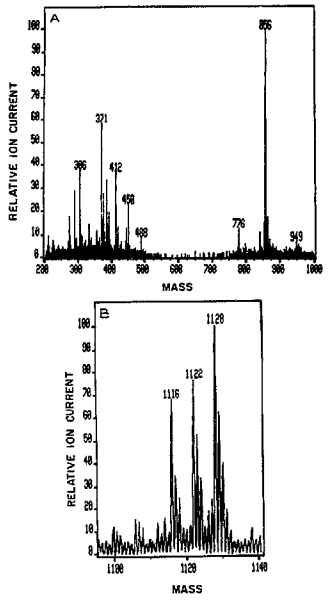

Fig. 2. Negative-ion fast atom bombardment-mass spectra of the underivatized compounds shown in Fig. 1. (A) The spectrum obtained from LY-Chol. The peak at mass 856 is the $[(M-Li+H)-Li^+]^-$ molecular ion for LY-Chol. The peaks at mass 450, corresponding to $[(M-Li+H)-H^+]^-$ for Lucifer yellow CH, and mass 412, corresponding to $[(M-Cl)-H^+]^-$ for cholesteryl chloroformate, may represent either fragment ions of LY-Chol or impurities in the preparation. The peak at mass 776, corresponding to $[(M-Li-SO_3+H)-Li^+]^-$ for LY-Chol, may indicate incomplete sulfonation during the synthesis of Lucifer yellow CH [26]. The other peaks in the spectrum were not assigned. (B) The spectrum obtained from LY-$DC_{12:0}$PE by multichannel averaging. The peaks at masses 1128, 1122, and 1116 are the $[M-H^+]^-$, $[(M-Li+H)-H^+]^-$, and $[(M-2Li+2H)-H^+]^-$ molecular ions, respectively, for LY-$DC_{12:0}$PE. Prominent peaks at lower mass in a conventional scan (not shown) include mass 946, corresponding to $[M-H^+]^-$ for lyso-LY-$DC_{12:0}$PE; mass 578, corresponding to $[M-H^+]^-$ for $DC_{12:0}$PE; and mass 396, corresponding to $[M-H^+]^-$ for lyso-$DC_{12:0}$PE.

shift toward longer wavelengths. The emission shifts are accompanied by reductions in both absorbance and quantum yield as the solvent polarity decreases (Table I).

Emission maxima at wavelengths more extreme than any of those reported in Table I are observed when the dyes are on TLC plates. As described in Materials and Methods, all four of the Lucifer yellow-lipid conjugates exhibit yellow fluorescence on wet K6F silica gel plates but orange fluorescence on dry plates. Because the solvent evaporates very rapidly once the plates are removed from the TLC chamber, it was not possible to obtain spectra from wet plates. On KC18F reversed-phase plates, however, the probes emit yellow fluorescence under either wet or dry conditions. Thus, it was possible to compare spectra of the yellow- and orange-emitting forms by comparing results from dry KC18F and dry K6F plates. These spectra were recorded by cutting the TLC plates to fit in the spectrofluorometer such that the excitation beam was perpendicularly incident on the desired spot. Fluorescence was collected at an angle of 22.5° relative to the excitation beam. The excitation and emission maxima of LY-Chol were found to be 424 nm and 511 nm, respectively, on reversed-phase plates and 428 nm and 592 nm, respectively, on silica gel plates. Similar shifts were observed with LY-$DC_{18:2}$PE for which the excitation and emission maxima were 425 nm and 511 nm, respectively, on reversed-phase plates and 434 nm and 574 nm, respectively, on silica gel plates (spectra not shown).

Since none of the four Lucifer yellow-lipid probes forms a true solution in water, this solvent is not listed in Table I. The probe that most closely approaches solubility in water is LY-Chol. Absorption scans of LY-Chol in isopropanol/water (1:1, v/v) fall to zero baseline at wavelengths longer than 500 nm. With LY-Chol in water, however, the absorption spectrum shows an appreciable baseline beyond 500 nm, indicating light scattering from micelles or other aggregates of LY-Chol. The temperature dependence of fluorescence intensity from a stable dispersion of LY-Chol in water is shown in Fig. 3. When presented in the format of an Arrhenius plot, the data is linear over a temperature range from

TABLE I

Spectral properties of LY-Chol and LY-$DC_{18:2}$PE in various solvents

Solvent	Absorption		Emission	
	λ_{max} (nm)	relative absorbance	λ_{max} (nm)	quantum yield
LY-Chol				
DMSO	435	1.00	517	0.63
Methanol	425	0.97	524	0.51
Isopropanol	429	0.93	517	0.52
Dioxane	432	0.56	582	0.062
LY-$DC_{18:2}$PE				
DMSO	435	1.00	521	0.55
Methanol	427	1.00	530	0.41
Isopropanol	436	0.49	534	0.14
Dioxane	434	0.48	562	0.073

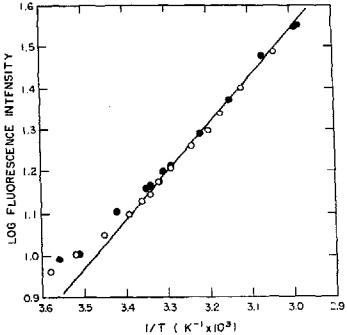

Fig. 3. Arrhenius plot of temperature dependence of integrated fluorescence intensity from a 0.2 mg/ml solution of LY-Chol in water. The excitation wavelength was 420 nm, and the fluorescence was collected at an angle of 22.5° relative to the excitation beam. Data are shown from both increasing (closed circles) and decreasing (open circles) temperature scans.

about 25 to 62°C. Deviation from linearity at lower temperatures may indicate the occurrence of a thermodynamic change in the range of 22 to 25°C. While the intensity of fluorescence is quite temperature dependent, the wavelength is not. The emission maximum appears at 539 nm at 6°C and shifts only slightly to 536 nm at 62°C.

Excitation and emission spectra are shown in Fig. 4 for LY-Chol incorporated at low level into the membranes of multilamellar lipid vesicles. Spectra obtained for LY-$DC_{16:0}$PE and LY-$DC_{18:2}$PE under these conditions (not shown) had nearly the same shape as those shown in Fig. 4. All three probes exhibited the emission maximum at 532 nm. The excitation maximum was at 425 nm for LY-Chol and at 427 nm for both LY-$DC_{16:0}$PE and LY-$DC_{18:2}$PE. Time-resolved fluorescence emission was also measured from these vesicle preparations to determine the fluorescence lifetimes of the lipid probes. Fitting the data (not shown) to single exponential decays yielded lifetimes of 7.4 ns for LY-Chol, 7.2 ns for LY-$DC_{16:0}$PE, and 7.6 ns for LY-$DC_{18:2}$PE. Since fitting the data to double exponential decays resulted in relative intensities of only 5% or less for the second components, the emissions appeared to be adequately described as due to single components.

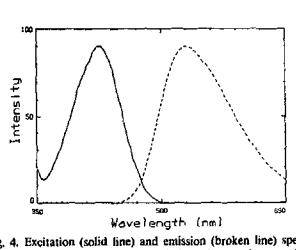

Fig. 4. Excitation (solid line) and emission (broken line) spectra of LY-Chol incorporated at 0.05 mol% into the membranes of multilamellar vesicles of $DC_{14:0}PC$/cholesterol (95:5, mol/mol). Spectra were recorded with total lipid concentration of 0.67 mg/ml in a phosphate buffer and with the fluorescence collected at an angle of 22.5° relative to the excitation beam. Temperature was 26°C.

Labeling cells with the probes

Human erythrocytes were labeled with 50 μg/ml LY-Chol, 400 μg/ml LY-$DC_{18:2}$PE, or 400 μg/ml LY-$DC_{16:0}$PE, and then lysed and washed to obtain ghosts. When examined under the fluorescence microscope, all three ghost preparations showed the ring pattern of fluorescence that is characteristic of plasma membrane labeling. Although all three probes could be incorporated into the membrane, the intensity of fluorescence labeling was much greater with LY-Chol than with the other two probes, in spite of the lower concentration of LY-Chol applied during labeling. As judged from the exposures required to produce micrographs of comparable brightness (not shown), the intensity of fluorescence from the LY-Chol ghosts was at least twice that from LY-$DC_{18:2}$PE ghosts and three times that from LY-$DC_{16:0}$PE ghosts. The extent of LY-Chol incorporation into the membrane was quanti-

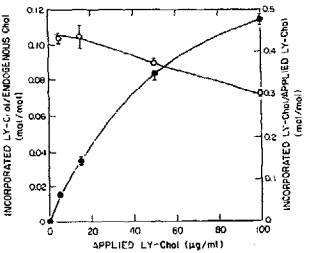

Fig. 5. Quantitation of incorporation of LY-Chol into the erythrocyte membrane. LY-Chol was added to washed erythrocytes (0.15 hematocrit) to obtain the indicated concentration, and then labeling was allowed to proceed for 20 min at 24°C before ghosts were isolated. Incorporation of LY-Chol is expressed relative to the amount of endogenous cholesterol in the membrane (closed circles). A significant fraction of the applied LY-Chol was actually incorporated into the membranes under these conditions (open circles).

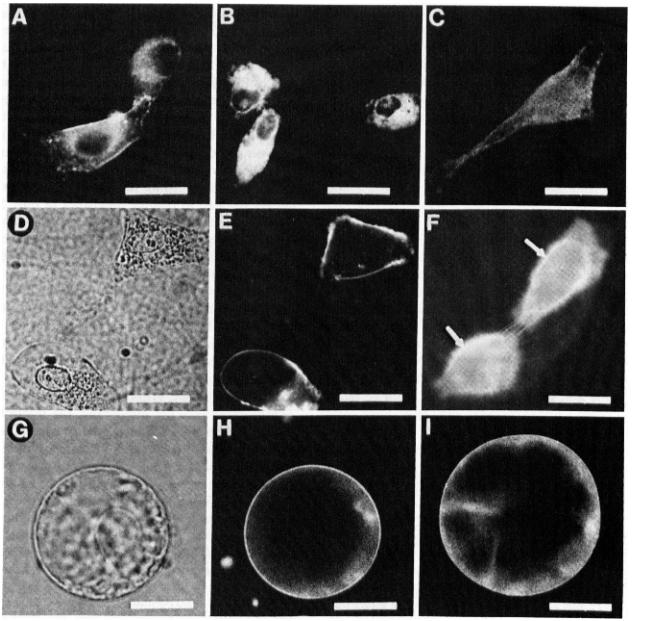

Fig. 6. Labeling of live amelanotic melanoma cells (A–F) and maize protoplasts (G–I) with fluorescent lipid probes. Paired brightfield and fluorescence micrographs are shown in (D) and (E) and also in (G) and (H). All other photographs are fluorescence micrographs. Labeling for 20 min at 26°C was with (A) 10 μg/ml NBD-PC, (B) 200 μg/ml LY-$DC_{18:2}$PE, (C) 200 μg/ml LY-$DC_{16:0}$PE, (E), 50 μg/ml LY-Chol, (F) 10 μg/ml LY-Chol, (H) and (I) 50 μg/ml LY-Chol. Micrographs (A–F) were recorded 55 to 115 min after the wash at the end of the labeling period, while (G–I) were recorded 3 h after the wash. Strong internalization of the fluorophores to the cytoplasm is evident in (A) and (B), with markedly less internalization in (E), (H), and (I). Photographic printing of (F) was done at very low contrast to enable visualization of the hair-like processes between and around the cells. The arrows in (F) point to the plasma membranes at the borders of the cells. Bars, 30 μm in (A–F) and 20 μm (G–I).

ıated relative to the amount of endogenous cholesterol in the membrane. The results (Fig. 5) show that remarkably high levels (11 mol%) of LY-Chol can be incorporated into the erythrocyte membrane. Significant depletion of the applied LY-Chol from the medium further indicates ready partitioning of LY-Chol into the membrane (Fig. 5).

Results of labeling experiments with live tissue culture cells and plant protoplasts are shown in Fig. 6. All of these micrographs were recorded after the cells or protoplasts had been allowed to incubate 1 h or longer after labeling to enable evaluation of the propensity for internalization. As expected on the basis of other reports [4,15,23,24], strong internalization of NBD-PC is observed under these conditions (Fig. 6A). Internalization of LY-$DC_{18:2}$PE (Fig. 6B) is also strong and results in an even lower ratio of surface- to internalized-fluorescence than occurs with NBD-PC. Internalization is more moderate with LY-$DC_{16:0}$PE, although membrane labeling is weak with this probe (Fig. 6C). In contrast to the other probes, LY-Chol exhibits very low internalization, as is evident from the very low level of perinuclear fluorescence (Fig. 6E). When viewed through the microscope, or when photographically

TABLE II

Lateral diffusion properties of lipid probes in various membranes

Probe	Membrane	Temp. [a] (°C)	Diffusion coefficient [b] (cm^2/s)	Mobile fraction [b]
LY-Chol	$DC_{12:0}PC$ [c]	10	$(1.6 \pm 0.8) \cdot 10^{-8}$	1.00 ± 0
LY-$DC_{18:2}$PE	$DC_{12:0}PC$ [c]	10	$(1.3 \pm 0.3) \cdot 10^{-8}$	0.99 ± 0.02
LY-Chol	$DC_{16:0}PC$ [d]	10	$(2.0 \pm 0.5) \cdot 10^{-11}$	0.87 ± 0.18
LY-$DC_{18:2}$PE	$DC_{16:0}PC$ [d]	10	$(5.6 \pm 3.4) \cdot 10^{-11}$	1.00 ± 0
LY-Chol	$DC_{12:0}PC/DC_{16:0}PC$ [e]	10	$(1.3 \pm 0.4) \cdot 10^{-9}$	1.00 ± 0
LY-$DC_{18:2}$PE	$DC_{12:0}PC/DC_{16:0}PC$ [e]	10	$(1.6 \pm 0.5) \cdot 10^{-9}$	0.91 ± 0.13
LY-Chol	$DC_{14:0}PC$/cholesterol [f]	26	$(1.5 \pm 0.2) \cdot 10^{-8}$	1.00 ± 0
LY-$DC_{18:2}$PE	$DC_{14:0}PC$/cholesterol [f]	26	$(2.2 \pm 1.3) \cdot 10^{-8}$	0.95 ± 0.07
LY-Chol	Erythrocyte ghost	26	$(1.8 \pm 0.5) \cdot 10^{-9}$	0.92 ± 0.09
diO	Erythrocyte ghost	26	$(2.4 \pm 0.4) \cdot 10^{-9}$	0.90 ± 0.06
NBD-PC	Melanoma cell	26	$(2.8 \pm 0.1) \cdot 10^{-9}$	0.72 ± 0.02
LY-$DC_{16:0}$PE	Melanoma cell	26	$(1.7 \pm 0.5) \cdot 10^{-9}$	0.46 ± 0.11
LY-Chol	Melanoma cell	26	$(1.8 \pm 0.1) \cdot 10^{-9}$	0.53 ± 0.03
LY-Chol	Melanoma cell	10	$(1.2 \pm 0.4) \cdot 10^{-9}$	0.39 ± 0.02

[a] Temp, temperature.
[b] Average ± S.D.
[c] Known to be fluid phase at 10 °C [3,42].
[d] Known to be gel phase at 10 °C [3,42].
[e] (1:1, mol/mol), known to be phase separated in sub-micrometer domains at 10 °C [3,42].
[f] (9:1, mol/mol), known to be fluid phase at 26 °C [12].

printed at very low contrast, amelanotic melanoma cells are seen to be covered with many hair-like processes that are readily labeled by LY-Chol (Fig. 6F). Labeling of maize protoplasts also results in a high ratio of surface fluorescence to internalized fluorescence (Fig. 6H). Internalization is evident in some protoplasts (Fig. 6I) and appears to involve dye movement into the transvacuolar strands.

Lateral diffusion properties of the probes

A survey of lateral diffusion characteristics of the Lucifer yellow-lipid conjugates in a variety of membranes is summarized in Table II. Multilamellar lipid vesicles of known phase properties were used as model systems to test the lateral diffusion characteristics of LY-Chol and LY-$DC_{18:2}$PE. Both of these probes exhibited rapid ($> 10^{-8}$ cm^2/s) diffusion in fluid phase membranes and very slow ($< 10^{-10}$ cm^2/s) diffusion in gel phase membranes, as expected. Intermediate diffusion rates (10^{-9} cm^2/s) were observed in membranes of mixed phase (Table II).

Diffusion coefficients in the range of 10^{-9} cm^2/s were measured both in ghost membranes from erythrocytes and in the plasma membranes of live amelanotic melanoma cells (Table II). While mobile fractions were near 1 for diffusion of the probes in both the lipid vesicles and in the erythrocyte ghosts, the mobile fractions were significantly less than 1 for diffusion in the plasma membrane of the melanoma cells. The mobile fraction of LY-Chol in the membrane was decreased by a decrease in temperature from 26 °C to 10 °C (Table II).

Discussion

Lucifer yellow-conjugates of both cholesterol and phosphatidylethanolamines can be prepared by single-step reactions and then purified by solvent partitioning. The relatively low final yields (typically 26%) of the phospholipid conjugates were due at least in part to the decision to sacrifice some of the material during solvent partitioning in order to obtain a purer final product (see Materials and Methods). If a more efficient purification technique, say high performance liquid chromatography, had been available, then it is likely that the final yields of LY-$DC_{12:0}$PE and the other phospholipid derivatives would have been significantly higher. Furthermore, analysis by TLC revealed that appreciable levels of contaminants were present in the commercial preparations of both Lucifer yellow CH and Lucifer yellow VS. Since these contaminants did not seem to interfere with the syntheses of the lipid probes, the commercial preparations were used without further purification. The presence of the contaminants does, however, reduce the theoretical and actual yields of the syntheses.

It is interesting to note that the emission maxima from solutions of LY-Chol and LY-$DC_{18:2}$PE shift to longer wavelengths as solvent polarity decreases (Table I), while on TLC plates the longer wavelengths of

emission are observed on the more polar K6F silica gel plates. These observations may indicate that the shift of emission to longer wavelengths in solution is due to dye–dye interactions rather than to dye–solvent interactions [1]. Dye–dye interactions or aggregation in nonpolar solvents would be consistent with the precipitous drops in quantum yield and absorbance under these conditions (Table I).

The increase in fluorescence intensity with temperature for LY-Chol in water (Fig. 3) probably also involves dye–dye interaction. Two general classes of fluorescence quenching, static and dynamic, can be distinguished by the temperature dependence of quenching [1]. Fluorescence increase with increasing temperature, such as shown in Fig. 3, is characteristic of static quenching [1]. Static quenching in this case probably arises from dye–dye interactions in micelles or other aggregates. As the temperature increases, LY-Chol becomes more soluble, and the aggregates probably begin to decrease in size. If dye aggregation at lower temperature is involved in this case, however, the aggregates must be different from those that seem to occur in nonpolar solvents, since no appreciable shift of emission occurs as the temperature of the aqueous dispersion is lowered.

Although LY-$DC_{16:0}$PE and LY-$DC_{18:2}$PE do label erythrocyte membranes, the labeling is not as intense as that achieved with LY-Chol. LY-Chol can be readily incorporated into erythrocyte membranes at remarkably high levels (Fig. 5), and also intensely labels melanoma cells and maize protoplasts (Fig. 6E, F, H, I). The ready insertion of LY-Chol into cell membranes contrasts with the difficult insertion reported for a different fluorescent cholesterol derivative [14].

When applied to live cells, LY-$DC_{18:2}$PE seems to exhibit much more internalization to the cytoplasm than does LY-$DC_{16:0}$PE (Fig. 6B, C). If these probes are metabolized and removed from the membrane as has been reported for some other fluorescent lipid probes [23,24], then the unsaturated fatty acyl chains of LY-$DC_{18:2}$PE would seem to promote the metabolic turnover of this probe. More rapid turnover of unsaturated than saturated phospholipids has been reported for plant cells [43].

LY-Chol exhibits remarkably slow internalization to the cytoplasm of both melanoma cells (Fig. 6E) and maize protoplasts (Fig. 6H, I). Some factors that may contribute to the slow internalization in protoplasts can be considered. LY-Chol carries two strong electrical charges that reduce the likelihood of passage through the hydrophobic region of the membrane. Furthermore, since these charges are negative, the electrochemical potential across the protoplast plasma membrane works to prevent internalization of LY-Chol. Finally, the plasma membrane contains a relatively higher proportion of sterols than do the endomembranes of plant cells [44,45]. Thus, metabolic processes may favor retention of LY-Chol in the plasma membrane rather than internalization to the endomembranes.

The lateral diffusion characteristics of LY-Chol and LY-$DC_{18:2}$PE in a variety of multilamellar lipid vesicles (Table II) are similar to the diffusion characteristics reported for other fluorescent lipid probes in these membranes [3,12]. Schneider et al. [46] have shown for other probes, however, that diffusion coefficients measured in the range of 10^{-11} cm^2/s for gel phase lipid probably represent diffusion along defects rather than diffusion in the ordered lipid. Hence, the true diffusion rates of LY-Chol and LY-$DC_{18:2}$PE in ordered gel-phase lipid are probably several orders of magnitude slower than reported in Table II.

As reported in Table II, LY-Chol and diO exhibit similar diffusion characteristics in erythrocyte membranes. These results are in good agreement with diffusion results reported for other lipid probes in erythrocyte membranes [14,47]. Likewise, the diffusion coefficients of LY-Chol and LY-$DC_{16:0}$PE in the membrane of melanoma cells are similar to diffusion coefficients reported for other fluorescent lipid probes in mammalian cells [4,15,48]. The mobile fractions of LY-Chol and LY-$DC_{16:0}$PE in the melanoma membrane are comparable to some reported mobile fractions [15,48] but are lower than others [4,15]. In short, the diffusion characteristics of LY-Chol, LY-$DC_{18:2}$PE, and LY-$DC_{16:0}$PE in these test systems appear to be comparable to results obtained by others working on similar systems with other fluorescent lipid probes.

It is worth noting that a concern may arise from the syntheses of these Lucifer yellow-lipid conjugates as the dilithium salts (Fig. 1). Lithium has been shown to be a reversible inhibitor of *myo*-inositol-1-phosphatase, with 50% inhibition of the enzyme occurring in the presence of 0.8 mM LiCl [49]. Since LY-Chol achieves high levels of labeling when applied at concentrations that involve much less than 0.8 mM lithium (Fig. 5), the resulting inhibition of the phosphatase should be minimal. In work where even slight inhibition of the enzyme is a concern, however, it may be necessary to exchange the lithium for another cation.

The goal of this work was to develop fluorescent lipid probes that would readily insert into the plasma membrane of live cells and then remain localized there with relatively little internalization to the cytoplasm. The synthesis and characterization of LY-Chol appears to fulfill this goal.

Acknowledgements

The author thanks Esther Valdez and Irwin W. Sherman for providing erythrocytes and tissue culture cells; David A. Johnson for performing the fluorescence lifetime measurements; William Okamura for assisting in

determining nomenclature for the new probes; Aileen Wietstruk for assistance in preparing the manuscript; and Rich Kondrat, Russ Tsao, and Ron New of the U.C.R. Mass Spectrometer Facility for obtaining the mass spectra. This work was supported by the U.S. Department of Agriculture Competitive Research Grants Program under grant 88-37264-3807, by the National Science Foundation Cell Biology Program under grant DCB-8716179, and by BRSG S07 RR07010-19 awarded by the Biomedical Research Support Grant Program, Division of Research Resources, National Institutes of Health.

References

1 Lakowicz, J.R. (1983) Principles of Fluorescence Spectroscopy, pp. 14–18, 139–142, 164–167, 188–295, Plenum Press, New York.
2 Dazko, Z. and Jacobson, K. (1980) Biochemistry 19, 6050–6057.
3 Klausner, R.D. and Wolf, D.E. (1980) Biochemistry 19, 6199–6203.
4 Struck, D.K. and Pagano, R.E. (1980) J. Biol. Chem. 255, 5404–5410.
5 Wolf, D.E., Kinsey, W., Lennarz, W. and Edidin, M. (1981) Dev. Biol. 81, 133–138.
6 Foley, M., MacGregor, A.N., Kusel, J.R., Garland, P.B., Downie, T. and Moore, I. (1986) J. Cell Biol. 103, 807–818.
7 Chattopadhyay, A. and London, E. (1988) Biochim. Biophys. Acta 938, 24–34.
8 Smutzer, G., Crawford, B.F. and Yeagle, P.L. (1986) Biochim. Biophys. Acta 862, 361–371.
9 Rando, R.R., Bangerter, F.W. and Alecio, M.R. (1982) Biochim. Biophys. Acta 684, 12–20.
10 Knight, C.G. and Dugan, G.M. (1986) Biochim. Biophys. Acta 860, 159–164.
11 Kao, Y.J., Soutar, A.K., Hong, K.-Y., Pownall, H.J. and Smith, L.C. (1978) Biochemistry 17, 2689–2696.
12 Alecio, M.R., Golan, D.E., Veatch, W.R. and Rando, R.R. (1982) Proc. Natl. Acad. Sci. USA 79, 5171–5174.
13 Schroeder, F., Barenholz, Y., Gratton, E. and Thompson, T.E. (1987) Biochemistry 26, 2441–2448.
14 Golan, D.E., Alecio, M.R., Veatch, W.R. and Rando, R.R. (1984) Biochemistry 23, 332–339.
15 Metcalf III, T.N., Wang, J.L. and Schindler, M. (1986) Proc. Natl. Acad. Sci. USA 83, 95–99.
16 Lojewska, Z. and Loew, L.M. (1987) Biochim. Biophys. Acta 899, 104–112.
17 Spiegel, S., Schlessinger, J. and Fishman, P.H. (1984) J. Cell Biol. 99, 699–704.
18 Packard, B.S., Karukstis, K.K. and Klein, M.P. (1984) Biochim. Biophys. Acta 769, 201–208.
19 Kuhry, J.-G., Duportail, G., Bronner, C. and Laustriat, G. (1985) Biochim. Biophys. Acta 845, 60–67.
20 Sleight, R.C. and Pagano, R.E. (1984) J. Cell Biol. 99, 742–751.
21 Sleight, R.G. and Pagano, R.E. (1985) J. Biol. Chem. 260, 1146–1154.
22 Martin, O.C. and Pagano, R.E. (1987) J. Biol. Chem. 262, 5890–5898.
23 Pagano, R.E. and Sleight, R.G. (1985) Science 229, 1051–1057.
24 Dengler, L. and Boss, W.F. (1987) Plant Physiol. 83 (Suppl.), 58.
25 Stewart, W.W. (1981) Nature 292, 17–21.
26 Stewart, W.W. (1981) J. Am. Chem. Soc. 103, 7615–7620.
27 Spiegel, S., Wilchek, M. and Fishman, P.H. (1983) Biochem. Biophys. Res. Commun. 112, 872–877.
28 Furtula, V., Walko, R.M. and Nothnagel, E.A. (1987) Protoplasma 139, 117–129.
29 Spiegel, S. (1985) Biochemistry 24, 5947–5952.
30 Barak, L.S. (1981) Cytoskeleton-Membrane Interactions: A Fluorescence Study of (NBD-Phallacidin)-Actin Labeling and Low Density Lipoprotein-Receptor Complex Diffusion on Human Fibroblasts, pp. 141–142, Ph.D. Dissertation, Cornell University, Ithaca, NY.
31 Guilbault, G.G. (1973) Practical Fluorescence: Theory, Methods, and Techniques, pp. 11–14, Marcel Dekker, New York.
32 Weber, G., Teale, F.W.J. (1957) Trans. Faraday Soc. 53, 646–655.
33 Johnson, D.A. and Yguerabide, J. (1985) Biophys. J. 48, 949–955.
34 Axelrod, D., Koppel, D.E., Schlessinger, J., Elson, E. and Webb, W.W. (1976) Biophys. J. 16, 1055–1069.
35 Li, Q. and Nothnagel, E.A. (1988) Plant Physiol. 86, 429–434.
36 Bloom, J.A. and Webb, W.W. (1983) Biophys. J. 42, 295–305.
37 Fahey, P.F. and Webb, W.W. (1978) Biochemistry 17, 3046–3053.
38 Bennett, V. (1983) in Methods in Enzymology (Fleischer, S. and Fleischer, B., eds.), Vol. 96, pp. 313–324, Academic Press, New York.
39 Roelofsen, B. and Ott, P. (1981) in Membrane Proteins: A Laboratory Manual (Azzi, A., Brodbeck, U. and Zahler, P., eds.), pp. 43–49, Springer, New York.
40 Kates, M. (1972) in Laboratory Techniques in Biochemistry and Molecular Biology (Work, T.S. and Work, E., eds.), Vol. 3, Part II, pp. 360–361, American Elsevier, New York.
41 Gronwald, J.W. and Leonard, R.T. (1982) Plant Physiol. 70, 1391–1395.
42 Hui, S.W. and Parsons, D.F. (1975) Science 190, 383–384.
43 Brown, J.H., Lynch, D.V. and Thompson, J.E. (1987) Plant Physiol. 85, 679–683.
44 Yoshida, S. and Uemura, M. (1984) Plant Physiol. 75, 31–37.
45 Yoshida, S. and Uemura, M. (1986) Plant Physiol. 82, 807–812.
46 Schneider, M.B., Chan, W.K. and Webb, W.W. (1983) Biophys. J. 43, 157–165.
47 Thompson, N.L. and Axelrod, D. (1980) Biochim. Biophys. Acta 597, 155–165.
48 Packard, B.S., Saxton, M.J., Bissell, M.J. and Klein, M.P. (1984) Proc. Natl. Acad. Sci. USA 81, 449–452.
49 Hallcher, L.M. and Sherman, W.R. (1980) J. Biol. Chem. 255, 10896–10901.